DØ Note 5934-CONF

Version: 1.0

Search for the associated production of charginos and neutralinos in the like-sign dimuon channel with DØ RunIIb data.

Andrey Shchukin, Vladimir Goryachev, Alexey Popov

(Dated: May 22, 2009)

A search charginos and neutralinos has been performed in $p\bar{p}$ collisions recorded with the D0 detector. The final state with two like sign muons and missing transverse energy is considered. The dataset used in this analysis corresponds to $\approx 3fb^{-1}$ integrated luminosity. The preliminary limit on the chargino production cross section times branching ratio into trileptons has been set.

Preliminary Results

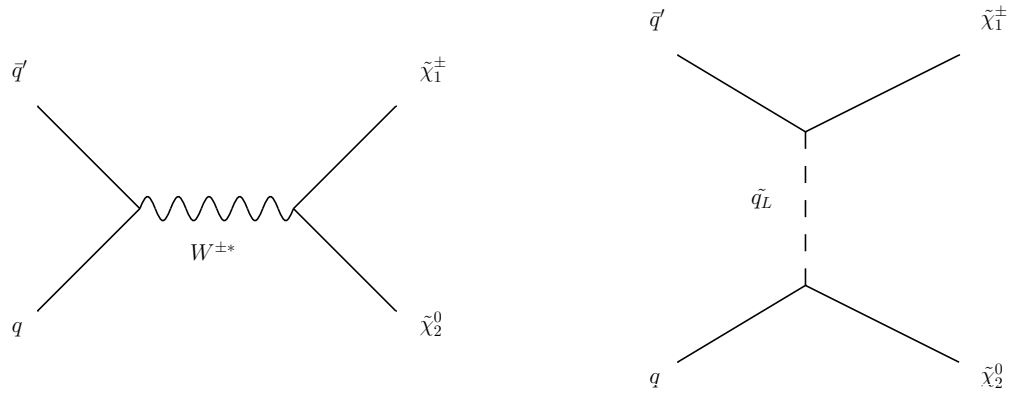

FIG. 1: $\tilde{\chi}_1^\pm$ $\tilde{\chi}_2^0$ production.

I. INTRODUCTION

Supersymmetry (SUSY) is a proposed symmetry between fermions and bosons and predicts the existence of supersymmetric partner for each standard model particle [1]. SUSY provides possible solutions to various standard model topics like hierarchy problem, unification of SU(3), SU(2), SU(1) gauge couplings, quantum gravity and the dark matter. Since we see only one half of the particles it means that supersymmetry must be broken at the electroweak scale. In the Minimal Supersymmetric extension of standard model (MSSM) this can be achieved by including explicitly soft SUSY terms into Lagrangian at electroweak scale, which are expected from a high energy breakdown of supersymmetry. The model which provides breaking mechanism is a minimal supergravity SUSY (mSUGRA) based on local supersymmetry requirements, where SUSY is broken in the ground state of hidden sector fields at GUT scale and mediated to the MSSM sector by gravity. This analysis is performed within mSUGRA framework. In R-parity conserving theories the supersymmetric particles (sparticles) are produced in pairs from $p\bar{p}$ collisions, then $\tilde{\chi}_1^0$ which is a stable lightest supersymmetric particle escapes the detection leading to significant missing transverse energy.

The associated production of the chargino $\tilde{\chi}_1^\pm$ and neutralino $\tilde{\chi}_2^0$ leads to trilepton final state. Such production can be performed via off-shell W boson or via squark exchange in t channel. The graphs for $\tilde{\chi}_1^\pm/\tilde{\chi}_2^0$ production are presented on Fig. 1. The graphs for chargino and neutralino decays are presented on Fig. 2.

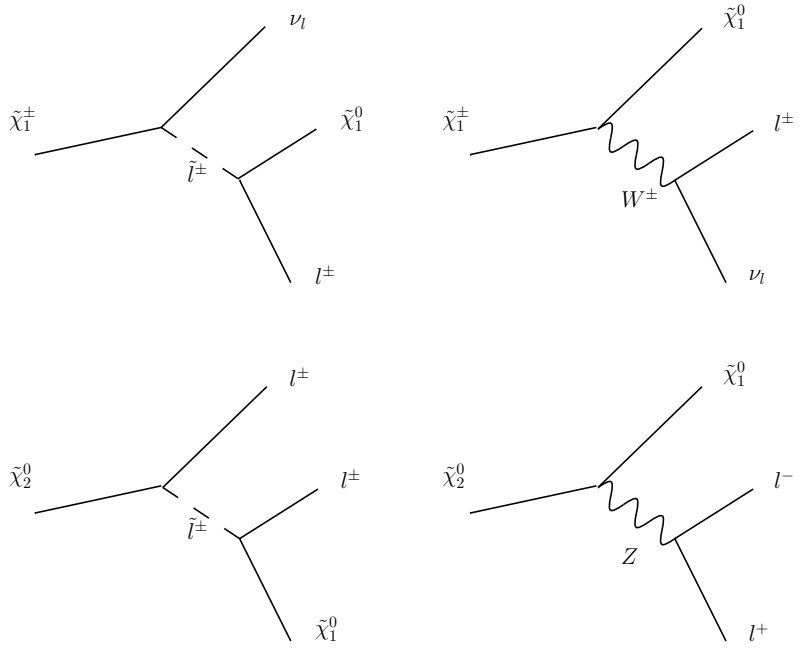

FIG. 2: $\tilde{\chi}_1^\pm$ and $\tilde{\chi}_2^0$ leptonic decays.

In the final state with three leptons and missing transverse energy the third lepton can be very soft (especially when slepton-neutralino mass difference is small) and this leads to like sign dimuon signature.

Previous searches in like sign channel at DØ have set limit on the associated production of $\tilde{\chi}_1^{\pm}$ and $\tilde{\chi}_2^0$ [2], [3] and were combined with trilepton results [4].

II. DATA AND MONTE CARLO SAMPLES

This search is performed on the data collected from June 9 2006 to December 11 2008 by the DØ detector [5] at the Fermilab Tevatron $p\bar{p}$ collider at a center of mass energy of 1.96 TeV and corresponds to an integrated luminosity 2976 pb^{-1}. The luminosity is calculated by normalizing Monte Carlo to data around $Z \to \mu\mu$ peak, using the NNLO cross section of 241.6 pb.

Signal Monte Carlo is produced with Pythia 6.319 with LHA input produced with SOFTSUSY 1.9.1. Cross sections are calculated using PROSPINO 2, with SUSY spectra determinated by SOFTSUSY 2.0.14. The branching ratio is calculated using PYTHIA 6.323. Both signal and standard model background Monte Carlo have been generated using CTEQ6L1 parton distribution functions. Then they were processed with full detector simulation. Signal parameter combinations have been generated for $A_0 = 0$, $tan\beta = 3$, $\mu > 0$ and chargino masses in the range of 112-168 GeV, see Table I. Major sources of background are $W \to \mu\nu$, $Z/\gamma^* \to \mu\mu$ and multijet background from QCD production. Multijet background was estimated from data as described in Section III. The trigger efficiency is taken into account by comparing the p_T distributions in Z/γ^* events in data and Monte Carlo.

TABLE I: Parameters of generated SUSY points.

Point [GeV]	m_0 [GeV]	$m_{1/2}$ [Gev]	$m(\tilde{\chi}_1^0)$ [GeV]	$m(\tilde{\chi}_1^+)$ [GeV]	$m(\tilde{l_R})$	$\sigma \times BR(3l)$ [pb]
1	77	183	119	116	111	0.4891
2	78	182	118	115	111	0.4800
3	79	181	117	115	111	0.4590
4	80	180	116	114	112	0.4232
5	81	180	116	114	113	0.3917
6	82	179	116	113	113	0.3458
7	83	178	115	112	114	0.2826
8	102	211	143	142	135	0.1714
9	103	210	142	141	136	0.1637
10	104	210	142	141	136	0.1556
11	105	209	141	140	137	0.1441
12	106	208	140	139	137	0.1283
13	107	207	139	139	138	0.0985
14	108	206	139	138	139	0.0245
15	126	240	168	168	160	0.0567
16	128	239	167	167	161	0.0517
17	129	238	166	166	162	0.0482
18	131	236	164	164	163	0.0277

III. EVENT SELECTION

Selected events are required to pass a set of triggers and to have two like sigh muons matched to central tracks with $p_T > 5$ GeV. Each muon must pass anti-cosmic cuts: time between scintillator hits must be in ± 10 ns range; distance of closest approach to the best primary vertex <0.16 cm. Δz between muon and primary vertex and Δz between two muons are required to be less than 1 cm. Number of CFT hits on muon track must be > 8. Two variables are used to check if a muon is isolated in the calorimeter and tracker:

- $E_T^{0.1<\Delta R<0.4}$ - the sum of the energy depositions in calorimeter cells in the hollow with $0.1 < \Delta R < 0.4$;
- $p_T^{R<0.5}$ - the sum of the transverse momenta of all tracks in the tracker in cone with radius $R = 0.5$,

where $R = \sqrt{\Delta\eta^2 + \Delta\phi^2}$.

The multijet background has been estimated from data as follows. Muons coming from the signal tend to be more isolated than those from multijet background processes. Two sample are formed from data using selection criteria but with two wo different isolation requirements::

- sample $\mathcal{S}$: both muons are tightly isolated;
- sample $\mathcal{Q}$: one muon is tightly isolated and second muon is loosely isolated .

The multijet background dominates in the region with high values of $\Delta\phi$. The region of $\Delta\phi > 2.9$ is chosen for normalization. Normalization factor is measured as function of p_T of loosely isolated muon by calculating the ratio of number of events in each bin of p_T distributions of $\mathcal{S}$ and $\mathcal{Q}$ samples:

$$R(p_T) = \frac{1}{2}\frac{S(p_T)}{Q(p_T^{looseisolated})}\Bigg|_{\Delta\phi>2.9} \tag{1}$$

The calculated normalization factor $R(p_T)$ fitted with exponential function is shown on the Fig. 3. The multijet background can be determined now as sample $\mathcal{Q}$ weighted with $R(p_T)$ in the region of $\Delta\phi < 2.9$. The cut $\Delta\phi < 2.9$ is fixed at pre-selection level. In addition to $R(p_T)$ jets multiplicity normalization has been performed.

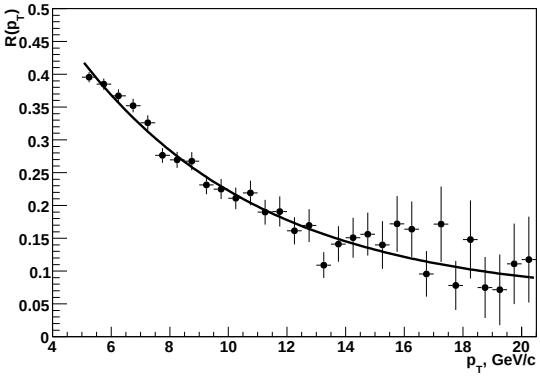

FIG. 3: Normalization function $R(p_T)$

In order to extract the signal events the selection criteria have been optimized to obtain the best expected limit on $\sigma(p\bar{p} \to \tilde{\chi}_1^{\pm}\tilde{\chi}_2^0) \times BR(3l)$. SUSY point 4 is used for optimization.

Transverse momenta (p_T), Fig. 4, 5. Cuts on the muons p_T is used to reject multijet background.

- $p_{T1} > 21GeV/c$;
- $p_{T2} > 10.5GeV/c$;
- $p_{T2} < 60GeV/c$;

Invariant mass of opposite sign pair, Fig. 6. If third muon is found in event then cut on $M_{OS} \in [10, 65]$ is applied. This cut rejects events Z/γ^*, WZ and ZZ events.

Invariant mass of like sign pair, Fig. 7. The cut on $M_{SS} \in [15, 120]$ is effective against W and WZ background.

Missing transverse energy $\not\!\!E_T$, Fig. 8. The $\tilde{\chi}_1^0$ produced in $\tilde{\chi}_1^{\pm}$ and $\tilde{\chi}_2^0$ decays is stable particle which escapes the detector leading to large amount of missing energy observed.

Significance of $\not\!\!E_T$, Fig. 9. Mismeasurements in the calorimeter can lead to artificial $\not\!\!E_T$. To remove this background, a significance of $\not\!\!E_T$ has been developed. This variable is defined as:

$$Sig(\not\!\!E_T) = \frac{\not\!\!E_T}{\sqrt{\sum E_{jet}\sigma^2_{proj}}} \tag{2}$$

where σ_{proj} is jet energy resolution projected onto $\not\!\!E_T$ direction. The requirement of $Sig(\not\!\!E_T) > 5.5$ is used in event selection.

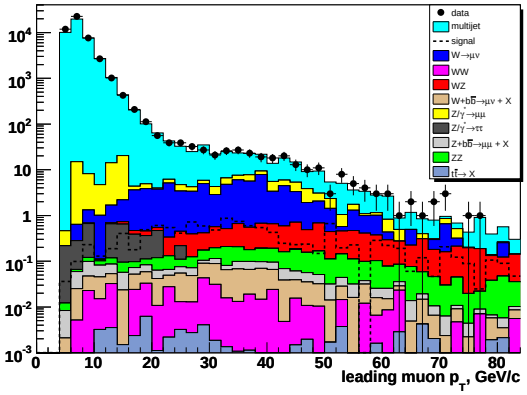

FIG. 4: Leading muon p_T at pre-selection level.

Transverse mass, Fig. 10. The cut on transverse mass $15 < M_{T2} < 80$ calculated using $\not{E}_T$ and p_T of next to leading muon is introduced to reject events from W and diboson background.

$$M_{T2} = \sqrt{2\,\not{E}_T \cdot p_{T2}(1 - cos\Delta\phi_{(\not{E}_T,\mu 2)})} \tag{3}$$

$\not{\mathbf{E}}_\mathbf{T} \times \mathbf{p_{T2}}$, Fig. 11. The cut of simple product $\not{E}_T \times p_{T2} > 500$ is effective against multijet background and background from W decays.

The number of events for data and background after each cut is listed in Table II.

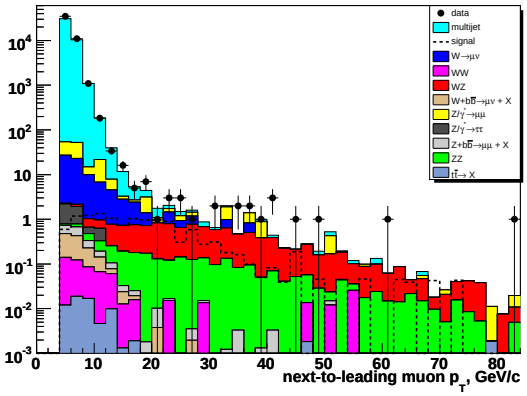

FIG. 5: Next to leading muon p_T at pre-selection level.

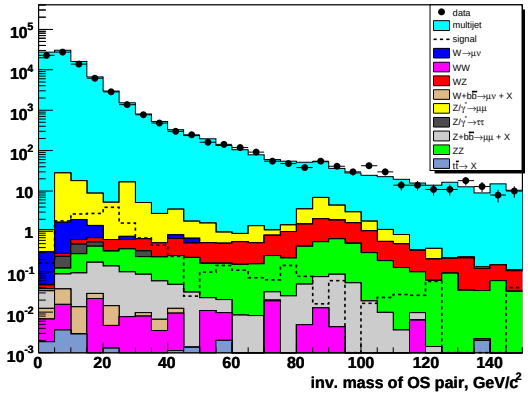

FIG. 6: Invariant mass of opposite sign muon pair at pre-selection level.

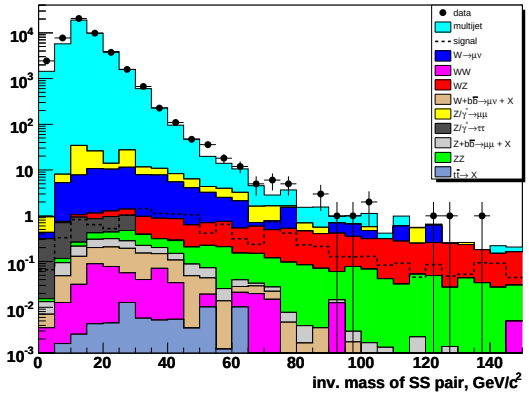

FIG. 7: Invariant mass of like sign muon pair at pre-selection level.

IV. SYSTEMATIC UNCERTAINTIES

The systematic uncertainties are coming from different sources such as detector simulation, modeling of the physics processes, multijet background estimation: luminosity uncertainty (6%), PDF uncertainty (¡4%), jet energy scale uncertainty (1%), muon identification and track matching systematics combined to 3% uncertainty, sign misidentification uncertainty (10%), multijet modeling uncertainty (30%).

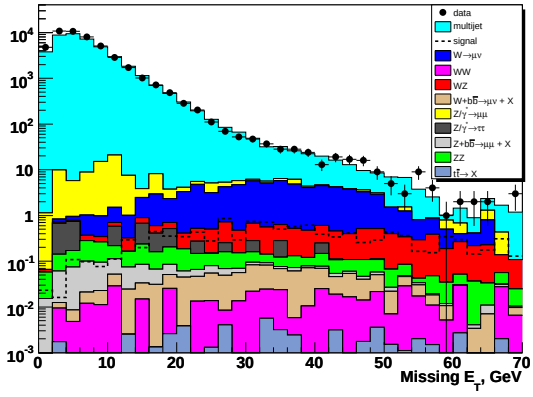

FIG. 8: Missing transverse energy at pre-selection level.

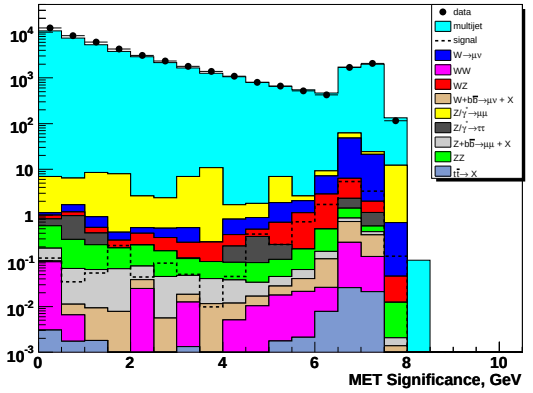

FIG. 9: Significance of missing transverse energy at pre-selection level.

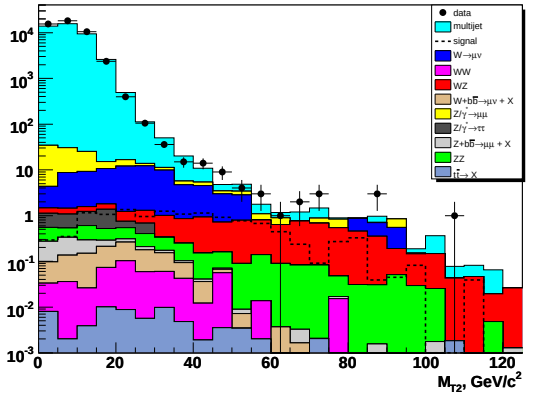

FIG. 10: Transverse mass computed using $\not{E}_T$ and p_{T2} at pre-selection level.

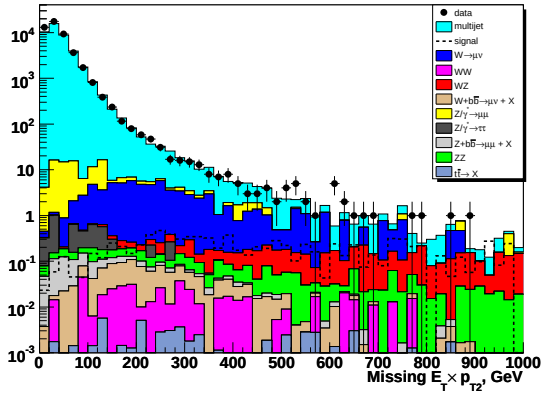

FIG. 11: Product of missing transverse energy and second muon p_T at pre-selection level.

TABLE II: Number of data and background events at different levels of selection

Cut	Multijet	$W \to \mu\nu$	$Z/\gamma^* \to \mu\mu$	WZ	WW	Wbb
Pre	43288 ± 141	70.3 ± 3.7	84.5 ± 12.3	10.2 ± 0.3	0.53 ± 0.07	0.90 ± 0.03
$10 < M_{OS} < 65$	23222 ± 105	69.1 ± 3.6	45.0 ± 8.1	4.0 ± 0.2	0.47 ± 0.07	0.87 ± 0.03
$p_{T2} < 60$	23222 ± 105	69.1 ± 3.6	44.9 ± 8.1	3.9 ± 0.2	0.46 ± 0.07	0.87 ± 0.03
$p_{T2} > 10.5$	90 ± 4	14.6 ± 2.2	9.4 ± 1.4	3.5 ± 0.2	0.18 ± 0.05	0.08 ± 0.01
$p_{T1} > 21$	13.8 ± 1.5	12.3 ± 2.0	7.2 ± 1.2	3.4 ± 0.2	0.16 ± 0.05	0.07 ± 0.01
$15 < M_{SS} < 120$	13.4 ± 1.5	11.6 ± 2.0	5.6 ± 1.1	2.8 ± 0.2	0.09 ± 0.04	0.07 ± 0.01
$15 < M_{T2} < 80$	7.9 ± 1.0	8.9 ± 1.7	3.9 ± 0.8	2.2 ± 0.1	0.08 ± 0.03	0.06 ± 0.01
$\not{E}_T > 25$	6.2 ± 1.0	7.7 ± 1.6	2.8 ± 0.6	1.8 ± 0.1	0.08 ± 0.03	0.05 ± 0.01
$Sig(\not{E}_T) > 5.5$	5.8 ± 1.0	7.7 ± 1.6	2.5 ± 0.6	1.8 ± 0.1	0.08 ± 0.02	0.05 ± 0.01
$\not{E}_T \times p_{T2} > 500$	2.1 ± 0.4	3.1 ± 0.9	1.3 ± 0.3	1.4 ± 0.1	0.07 ± 0.02	0.02 ± 0.01
Cut	ZZ	$t\bar{t}$	$Z/\gamma^* \to \tau\tau$	Zbb	$Sum(Bkg)$	$Data$
Pre	2.61 ± 0.11	0.07 ± 0.01	3.1 ± 0.7	0.73 ± 0.02	43461 ± 142	47000
$10 < M_{OS} < 65$	0.72 ± 0.06	0.06 ± 0.01	2.9 ± 0.7	0.37 ± 0.02	23345 ± 107	29030
$p_{T2} < 60$	0.69 ± 0.06	0.06 ± 0.01	2.9 ± 0.7	0.37 ± 0.02	23345 ± 107	29029
$p_{T2} > 10.5$	0.52 ± 0.05	0.01 ± 0.004	0.3 ± 0.3	0.05 ± 0.01	118.6 ± 4.8	118
$p_{T1} > 21$	0.43 ± 0.05	0.01 ± 0.004	0.01 ± 0.01	0.04 ± 0.01	37.4 ± 2.8	31
$15 < M_{SS} < 120$	0.37 ± 0.04	0.01 ± 0.004	0.01 ± 0.01	0.03 ± 0.01	33.9 ± 2.7	24
$15 < M_{T2} < 80$	0.27 ± 0.04	0.01 ± 0.004	0.01 ± 0.01	0.02 ± 0.01	23.4 ± 2.1	17
$\not{E}_T > 25$	0.20 ± 0.03	0.01 ± 0.004	0	0.01 ± 0.01	18.9 ± 1.9	15
$Sig(\not{E}_T) > 5.5$	0.17 ± 0.02	0.01 ± 0.004	0	0.009 ± 0.004	18.1 ± 1.8	15
$\not{E}_T \times p_{T2} > 500$	0.14 ± 0.4	0.01 ± 0.003	0	0.007 ± 0.004	8.1 ± 1.8	7

TABLE III: Number of signal events at different levels of selection. SUSY points 1-8.

Cut	1	2	3	4
Pre	15.04 ± 0.81	15.68 ± 0.81	13.84 ± 0.75	12.51 ± 0.70
$10 < M_{OS} < 65$	12.30 ± 0.74	13.51 ± 0.75	11.11 ± 0.68	10.09 ± 0.64
$p_{T2} < 60$	12.20 ± 0.73	13.46 ± 0.75	11.06 ± 0.67	9.96 ± 0.63
$p_{T2} > 10.5$	8.04 ± 0.64	9.36 ± 0.67	7.91 ± 0.61	7.49 ± 0.58
$p_{T1} > 21$	6.92 ± 0.59	8.03 ± 0.62	6.94 ± 0.57	6.72 ± 0.55
$15 < M_{SS} < 120$	6.73 ± 0.59	7.59 ± 0.60	6.33 ± 0.54	6.05 ± 0.52
$15 < M_{T2} < 80$	5.39 ± 0.53	6.75 ± 0.57	5.30 ± 0.50	5.25 ± 0.49
$\not{E}_T > 25$	4.58 ± 0.49	5.29 ± 0.50	4.54 ± 0.46	4.50 ± 0.45
$Sig(\not{E}_T) > 5.5$	4.52 ± 0.48	5.06 ± 0.49	4.35 ± 0.45	4.46 ± 0.45
$\not{E}_T \times p_{T2} > 500$	3.03 ± 0.40	4.22 ± 0.45	3.71 ± 0.42	4.02 ± 0.43
Cut	5	6	7	8
Pre	13.77 ± 0.71	14.86 ± 0.73	14.21 ± 0.63	6.37 ± 0.29
$10 < M_{OS} < 65$	11.96 ± 0.66	12.88 ± 0.68	13.48 ± 0.61	5.17 ± 0.26
$p_{T2} < 60$	11.96 ± 0.66	12.77 ± 0.68	13.37 ± 0.61	5.14 ± 0.26
$p_{T2} > 10.5$	9.50 ± 0.62	11.01 ± 0.65	11.49 ± 0.58	3.51 ± 0.23
$p_{T1} > 21$	8.82 ± 0.59	10.09 ± 0.62	10.27 ± 0.55	3.22 ± 0.22
$15 < M_{SS} < 120$	8.34 ± 0.58	9.49 ± 0.60	9.74 ± 0.54	3.07 ± 0.22
$15 < M_{T2} < 80$	7.09 ± 0.53	8.11 ± 0.55	8.49 ± 0.50	2.37 ± 0.19
$\not{E}_T > 25$	5.66 ± 0.47	6.63 ± 0.50	6.97 ± 0.46	1.96 ± 0.17
$Sig(\not{E}_T) > 5.5$	5.50 ± 0.47	6.45 ± 0.49	6.71 ± 0.45	1.94 ± 0.17
$\not{E}_T \times p_{T2} > 500$	4.81 ± 0.44	5.70 ± 0.47	5.79 ± 0.41	1.60 ± 0.16

TABLE IV: Number of signal events at different levels of selection. SUSY points 9-16.

Cut	9	10	11	12
Pre	5.43 ± 0.25	5.76 ± 0.26	5.75 ± 0.29	5.23 ± 0.24
$10 < M_{OS} < 65$	4.62 ± 0.24	5.03 ± 0.25	5.00 ± 0.27	4.61 ± 0.22
$p_{T2} < 60$	4.59 ± 0.24	4.95 ± 0.25	4.91 ± 0.27	4.51 ± 0.22
$p_{T2} > 10.5$	3.46 ± 0.22	3.75 ± 0.23	4.17 ± 0.26	3.87 ± 0.21
$p_{T1} > 21$	3.22 ± 0.21	3.52 ± 0.22	3.91 ± 0.25	3.75 ± 0.21
$15 < M_{SS} < 120$	2.94 ± 0.20	3.20 ± 0.21	3.50 ± 0.23	3.45 ± 0.20
$15 < M_{T2} < 80$	2.44 ± 0.18	2.50 ± 0.19	2.74 ± 0.21	2.74 ± 0.18
$\not{E}_T > 25$	1.98 ± 0.17	2.24 ± 0.18	2.52 ± 0.20	2.43 ± 0.17
$Sig(\not{E}_T) > 5.5$	1.90 ± 0.16	2.15 ± 0.17	2.46 ± 0.20	2.32 ± 0.16
$\not{E}_T \times p_{T2} > 500$	1.73 ± 0.15	1.99 ± 0.17	2.18 ± 0.19	2.16 ± 0.16
Cut	13	14	15	16
Pre	6.50 ± 0.26	1.76 ± 0.06	2.56 ± 0.11	2.30 ± 0.10
$10 < M_{OS} < 65$	5.97 ± 0.25	1.44 ± 0.05	2.04 ± 0.09	1.94 ± 0.10
$p_{T2} < 60$	5.85 ± 0.25	1.42 ± 0.05	1.99 ± 0.09	1.89 ± 0.10
$p_{T2} > 10.5$	5.21 ± 0.24	1.16 ± 0.05	1.49 ± 0.09	1.55 ± 0.09
$p_{T1} > 21$	5.01 ± 0.24	1.01 ± 0.05	1.41 ± 0.08	1.50 ± 0.09
$15 < M_{SS} < 120$	4.73 ± 0.23	0.94 ± 0.04	1.25 ± 0.08	1.31 ± 0.08
$15 < M_{T2} < 80$	3.75 ± 0.21	0.79 ± 0.04	0.90 ± 0.07	0.92 ± 0.07
$\not{E}_T > 25$	3.18 ± 0.19	0.66 ± 0.04	0.78 ± 0.06	0.83 ± 0.07
$Sig(\not{E}_T) > 5.5$	3.08 ± 0.19	0.64 ± 0.04	0.74 ± 0.06	0.79 ± 0.06
$\not{E}_T \times p_{T2} > 500$	2.71 ± 0.17	0.56 ± 0.03	0.69 ± 0.06	0.72 ± 0.06

TABLE V: Number of signal events at different levels of selection. SUSY points 17-18.

Cut	17	18
Pre	2.16 ± 0.10	1.75 ± 0.07
$10 < M_{OS} < 65$	1.81 ± 0.09	1.51 ± 0.06
$p_{T2} < 60$	1.75 ± 0.09	1.46 ± 0.06
$p_{T2} > 10.5$	1.50 ± 0.09	1.30 ± 0.06
$p_{T1} > 21$	1.43 ± 0.09	1.26 ± 0.06
$15 < M_{SS} < 120$	1.25 ± 0.08	1.13 ± 0.06
$15 < M_{T2} < 80$	0.90 ± 0.07	0.81 ± 0.05
$\not{E}_T > 25$	0.81 ± 0.06	0.71 ± 0.04
$Sig(\not{E}_T) > 5.5$	0.77 ± 0.06	0.66 ± 0.04
$\not{E}_T \times p_{T2} > 500$	0.72 ± 0.06	0.61 ± 0.04

V. RESULTS

7 events in data are consistent with expected background, no excess of SUSY events is observed. The limit on $\sigma(p\bar{p} \to \tilde{\chi}_1^{\pm}\tilde{\chi}_2^0) \times BR(3l)$ has been calculated for analyzed SUSY points using ROOT class TLimit based on CLS method [6]. Observed and expected limits as function of chargino mass are presented on Fig. 12. SUSY points 5, 7, 13, 19 are chosen (see Table I).

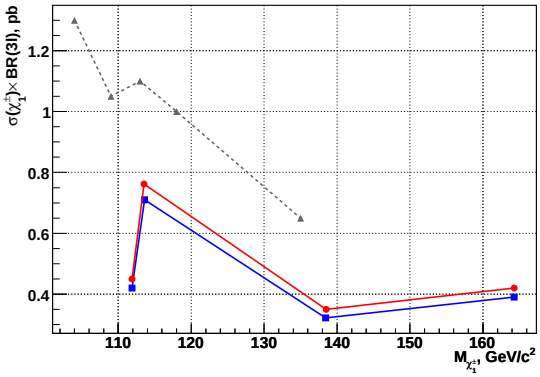

FIG. 12: Observed limit from previous result (line+triangles), observed (line+boxes) and expected (line+circles) limits on $\sigma(p\bar{p} \to \tilde{\chi}_1^{\pm}\tilde{\chi}_2^0) \times BR(3l)$.

The limits for different regions of $m_0 - m_{1/2}$ scan are shown on Fig. 13, 14, 15.

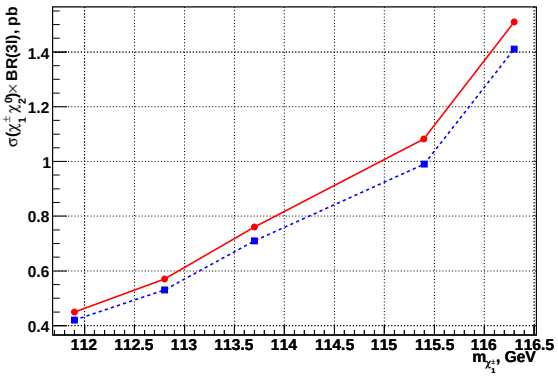

FIG. 13: Observed (dash line) and expected (solid line) limits on $\sigma(p\bar{p} \to \tilde{\chi}_1^{\pm}\tilde{\chi}_2^0) \times BR(3l)$. $m_0 = 77 - 83, m_{1/2} = 178 - 183$

VI. CONCLUSION

Preliminary results obtained in this analysis using $\approx 3fb^{-1}$ dataset show noticeable improvement compared to previous results [3]. This observed improvement is basically due to having more luminosity. The major source of uncertainty is multijet background modeling. The major sources of background are multijet background and $W \to \mu\nu$ decays. 7 events observed in this analysis are consistent with 8.1 ± 1.8 events expected from background. Further optimization of multijet background estimation as well as study of background from W events can lead to significant improvement of the quantity of $\sigma(p\bar{p} \to \tilde{\chi}_1^{\pm}\tilde{\chi}_2^0) \times BR(3l)$. Obtained results are to be combined with RunIIa data and with latest results of trilepton analysis [7].

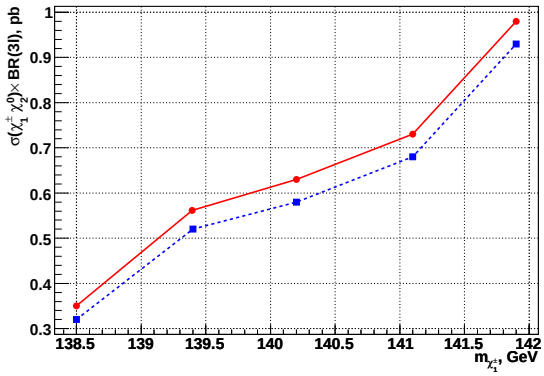

FIG. 14: Observed (dash line) and expected (solid line) limits on $\sigma(p\bar{p} \to \tilde{\chi}_1^{\pm}\tilde{\chi}_2^0) \times BR(3l)$. $m_0 = 101 - 108, m_{1/2} = 206 - 211$

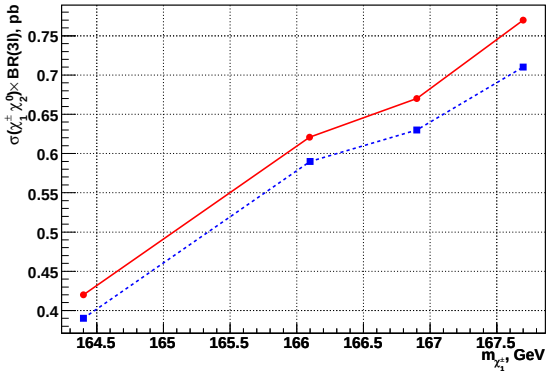

FIG. 15: Observed (dash line) and expected (solid line) limits on $\sigma(p\bar{p} \to \tilde{\chi}_1^{\pm}\tilde{\chi}_2^0) \times BR(3l)$. $m_0 = 126 - 131, m_{1/2} = 236 - 240$

Acknowledgments

We thank the staffs at Fermilab and collaborating institutions, and acknowledge support from the Department of Energy and National Science Foundation (USA), Commissariat à l'Energie Atomique and CNRS/Institut National de Physique Nucléaire et de Physique des Particules (France), Ministry of Education and Science, Agency for Atomic Energy and RF President Grants Program (Russia), CAPES, CNPq, FAPERJ, FAPESP and FUNDUNESP (Brazil), Departments of Atomic Energy and Science and Technology (India), Colciencias (Colombia), CONACyT (Mexico), KRF (Korea), CONICET and UBACyT (Argentina), The Foundation for Fundamental Research on Matter (The Netherlands), PPARC (United Kingdom), Ministry of Education (Czech Republic), Natural Sciences and Engineering Research Council and WestGrid Project (Canada), BMBF (Germany), A.P. Sloan Foundation, Civilian Research and Development Foundation, Research Corporation, Texas Advanced Research Program, and the Alexander von Humboldt Foundation.

---

[1] H.P. Nilles, Phys. Rep. 110 (1984) 1.
[2] A. Yurkewicz et al. D0 Note 4408.
[3] V. Lesne. D0 Note 5132.
[4] V. Abazov et al. (D0 Collaboration). *Search for supersymmetry via associated production of charginos and neutralinos in final states with three leptons*, Phys. Rev. Lett. 95 (2005) 151805.
[5] V. Abazov et al. (D0 Collaboration), *The Upgraded D0 Detector*, Nucl. Instrum. Meth. A, 546, 463(2006)
[6] G. Cowan. S*tatistical Data Analysis. Oxford University Press*, Oxford, New York, 1998.
[7] V. Abazov et al. (D0 Collaboration). *Search for Associated Production of Charginos and Neutralinos in the Trilepton Final State* Submitted to Phys. Lett. B, arXiv.org:0901.0646.